PHYSICAL REVIEW B, VOLUME 65, 144441

# Low-field hysteresis in disordered ferromagnets

Lorenzo Dante,[1] Gianfranco Durin,[2] Alessandro Magni,[2] and Stefano Zapperi[1]
[1]*INFM unità di Roma 1, Dipartimento di Fisica, Università "La Sapienza," P.le A. Moro 2, 00185 Roma, Italy*
[2]*Istituto Elettrotecnico Nazionale Galileo Ferraris and INFM, strada delle Cacce 91, I-10135 Torino, Italy*
(Received 18 December 2001; published 4 April 2002)

We analyze low-field hysteresis close to the demagnetized state in disordered ferromagnets using the zero-temperature random-field Ising model. We solve the demagnetization process exactly in one dimension and derive the Rayleigh law of hysteresis. The initial susceptibility $a$ and the hysteretic coefficient $b$ display a peak as a function of the disorder width. This behavior is confirmed by numerical simulations $d=2,3$ showing that in the limit of weak disorder demagnetization is not possible and the Rayleigh law is not defined. These results are in agreement with experimental observations on nanocrystalline magnetic materials.

DOI: 10.1103/PhysRevB.65.144441 PACS number(s): 75.60.Ej, 64.60.Ht, 68.35.Ct, 75.60.Ch

## I. INTRODUCTION

Ferromagnetic materials display hysteresis under the action of an external field and the magnetization depends in a complex way on the field history. In order to define magnetic properties unambiguously, it is customary to first *demagnetize* the material, bringing it to a state of zero magnetization at zero field. This can be done, in practice, by the application of a slowly varying ac field with decreasing amplitude. In this way, the system explores a complex energy landscape, due to the interplay between structural disorder and interactions, until it is trapped into a low-energy minimum. This demagnetized state is then used as a reference frame to characterize the magnetic properties of the material.

The hysteresis properties at low fields, starting from the demagnetized state, have been investigated already in 1887 by Lord Rayleigh,[1] who found that the branches of the hysteresis loop are well described by parabolas. In particular, when the field $H$ is cycled between $\pm H^*$, the magnetization $M$ follows $M=(a+bH^*)H\pm b[(H^*)^2-H^2]/2$, where the signs $\pm$ distinguish the upper and lower branch of the loop. Consequently, the area of the loop scales with the peak field $H^*$ as $W=4/3b(H^*)^3$ and the response to a small field change, starting from the demagnetized state, is given by $M^*=a(H^*)\pm b(H^*)^2$.[2]

The Rayleigh law has been widely observed in ferromagnetic materials,[2] but also in ferroelectric ceramics.[3,4] The current theoretical interpretation of this law is based on a 1942 paper by Néel,[5] who derived the law formulating the magnetization process as the dynamics of a point (i.e., the position of a domain wall) in a random potential. In this framework, the initial susceptibility $a$ is associated to reversible motions inside one of the many minima of the random potential, while the hysteretic coefficient $b$ is due to irreversible jumps between different minima. Successive developments and improvements have been devoted to establish precise links between Néel random potential and the material microstructure,[6–9] but in several cases the issue is still unsettled. For instance, the initial permeability of nanocrystalline materials typically displays a peak as a function of the grain size,[10] heat treatment,[11,12] or alloy composition.[10,13] This behavior can be associated with changes in the disordered microstructure, but cannot be accounted for by Néel theory that predicts a monotonic dependence of $a$ on the disorder width.[5]

The zero-temperature random-field Ising model (RFIM) has been recently used to describe the competition between quenched disorder and exchange interactions and their effect on the hysteresis loop.[14] In three and higher dimensions, the model shows a phase transition between a continuous cycle for strong disorder and a discontinuous loop, with a macroscopic jump, at low disorder. The two phases are separated by a second-order critical point, characterized by universal scaling laws.[14–16] A behavior of this kind is not restricted to the RFIM but has also been observed in other models, with random bonds or random anisotropies[17] and vectorial spins.[18] In addition, a similar disorder induced phase transition in the hysteresis loop has been experimentally reported for a Co-CoO bilayer.[19] Thus the RFIM provides a tractable model for a more generic behavior: the model has been solved exactly in one dimension[20,21] and on the Bethe lattice,[22,23] while mean-field theory[14] and renormalization group[15] have been used to analyze the transition.

Here, we use the RFIM to analyze the demagnetization process and investigate the properties of the hysteresis loop at low fields. Along the lines of Refs. 21 and 23, we compute the demagnetization cycles exactly in one dimension and derive the Rayleigh law, obtaining $a$ and $b$ as function of disorder and exchange energies. Next, we analyze the problem numerically in higher dimensions (i.e., $d=2$ and $d=3$) where exact results are at present not available. In $d=3$, we find that the disorder induced transition,[14] defined on the saturation loop, is also reflected by the Rayleigh loops: in the weak disorder phase the system cannot be demagnetized, as the final magnetization coincides with the saturation magnetization. A similar behavior has been recently obtained analyzing subloops.[24] In the high disorder phase, however, a demagnetization process is possible and hysteresis loops are still described by the Rayleigh law. Above the transition, the dependence of $a$ and $b$ on disorder is qualitatively similar in all dimensions, displaying a peak and decreasing to zero for very strong disorder in agreement with experiments.[10–13]

## II. RANDOM-FIELD ISING MODEL

In the RFIM, a spin $s_i=\pm 1$ is assigned to each site $i$ of a $d$-dimensional lattice. The spins are coupled to their nearest-

 

neighbor spins by a ferromagnetic interaction of strength $J$ and to the external field $H$. In addition, to each site of the lattice it is associated a random field $h_i$ taken from given probability distribution $\rho(h)$. In the following we will mainly focus on a Gaussian with variance $R$ [i.e., $\rho(h) = \exp(-h^2/2R^2)/\sqrt{2\pi}R$], but we will also consider a rectangular distribution. The Hamiltonian thus reads

$$\mathcal{H} = -\sum_{\langle i,j \rangle} J s_i s_j - \sum_i (H + h_i) s_i , \tag{1}$$

where the first sum is restricted to nearest-neighbors pairs. The dynamics proposed in Ref. 25 and used in Refs. 14–16 is such that the spins align with the local field

$$s_i = \mathrm{sgn}\left( J \sum_j s_j + h_i + H \right). \tag{2}$$

In $d=1$, a spin with $n$ neighbors *up* ($n=0,1,2$), will be *up* at the field $H$ with probability:

$$p_n(H) \equiv \int_{2(1-n)J-H}^{+\infty} \rho(h_i) dh_i . \tag{3}$$

When a spin flips *up* the local field of its neighbors is raised by $2J$ so that it can happen that one or both of the two neighbors flip *up*. In this way a single spin flip can lead the neighboring spins to flip, eventually triggering an avalanche.

It has been shown that the RFIM obeys return-point memory:[14] if the field is increased adiabatically the magnetization only depends on the state in which the field was last reversed. This property has been exploited in $d=1$ and in the Bethe lattice to obtain exactly the saturation cycle and the first minor loops.[21] In the next section we will briefly recall the results reported in Ref. 21 and we will then proceed with a general derivation for nested minor loops.

## III. SATURATION LOOP AND FIRST RETURN CURVES

To obtain the saturation loop, we start from the initial condition $s_i = -1$ at $H = -\infty$ and we will raise the field up to $H_0$. We are thus moving on the lower half of the major hysteresis loop. Following Ref. 21, we define the conditional probability $U_0$ that a spin flips *up* at $H_0$ before a given nearest neighbor. To compute $U_0$, we take advantage of the translational invariance of the system. There are only two ways to flip *up* a spin in $i$ keeping the spin in $i-1$ *down*. The two contributions yield $U_0 = p_1(H_0)U_0 + p_0(H_0)[1-U_0]$, from which we obtain

$$U_0 = \frac{p_0(H_0)}{1 - [p_1(H_0) - p_0(H_0)]}. \tag{4}$$

The probability that a spin is *up* at field $H_0$ is

$$p(H_0) = U_0^2 p_2(H_0) + 2U_0(1-U_0)p_1(H_0) + (1-U_0)^2 p_0(H_0) \tag{5}$$

and the magnetization per spin $M(H_0)$ is simply $M(H_0) = 2p(H_0) - 1$. In Fig. 1 we show the saturation loop for a Gaussian distribution of random fields.

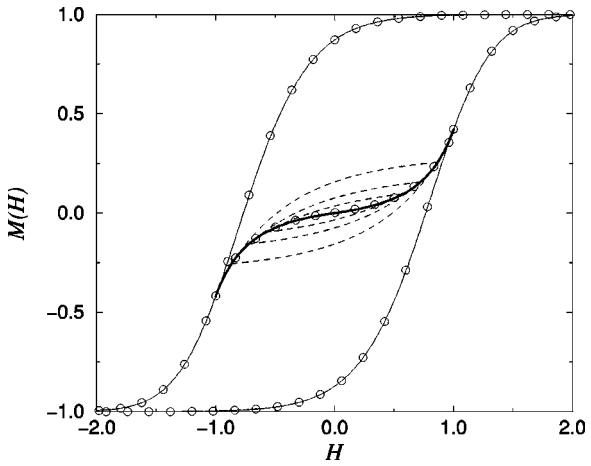


FIG. 1. Exact expressions for the saturation cycle (thin lines), the demagnetization curve (thick lines), and a few minor loops (dotted lines) for $J=1$ and $R=1$. The points are the results of a numerical simulation with $L=5\times10^5$ spins and a single realization of the disorder.

If the field is reversed from a finite value $H_0$, we have a new situation and the system departs from the saturation curve. It is possible to show that if the field changes from $H_0$ to $H_1 = H_0 - 2J$ the magnetization reaches the upper saturation loop again. Thus we can restrict the analysis to fields included in $[H_0 - 2J, H_0]$. The first return curve can be obtained counting the spins that were *up* at $H_0$ and are *down* at $H_1$. To this end, we introduce $D_1$ as the conditional probability that a spin is *down* if its neighbor is *up*. Following similar steps as for $U_0$,[21] we obtain

$$D_1 = \frac{f(H_0) + U_0[p_2(H_0) - p_2(H_1)]}{1 - [p_1(H_0) - p_1(H_1)]}, \tag{6}$$

where $f(H_0) \equiv U_0[1 - p_1(H_0)] + (1-U_0)[1 - p_2(H_0)]$. At this point it is straightforward to write the probability $p(H_1)$ that a spin is *up* at $H_1$:

$$p(H_1) = p(H_0) - (U_0^2[p_2(H_0) - p_2(H_1)] + 2U_0 D_1[p_1(H_0) - p_1(H_1)] + D_1^2[p_0(H_0) - p_0(H_1)]) \tag{7}$$

which is simply related to the magnetization.

## IV. DEMAGNETIZATION

Here, we extend the approach of Ref. 21 to more general field histories, treating explicitly the demagnetization process: the external field is changed through a nested succession $H = H_0 \to H_1 \to H_2 \to \cdots H_n \cdots \to 0$, with $H_{2n} > H_{2n+2} > 0$, $H_{2n-1} < H_{2n+1} < 0$, and $dH \equiv H_{2n} - H_{2n+2} \to 0$. The initial value $H_0$ should correspond to complete saturation, but we discussed above that as long as $H_n \geq J$ the magnetization $M_n \equiv M(H_n)$ simply follows the saturation curve, so that we can set $H_0 = J$.

As in the previous section, the key quantity to compute is

the conditional probability $U_{2n}$ that a spin flips up before its nearest neighbor when the field is increased from $H_{2n-1}$ to $H_{2n}$. Similarly on the descending part of the loops we define $D_{2n+1}$ as the conditional probability that a spin flips down before its nearest neighbor when the field is decreased from $H_{2n}$ to $H_{2n+1}$. Enumerating all possible spin histories, we find recursion relations for the conditional probabilities which read as[26]

$$\begin{cases} U_{2n}=U_{2n-2}+\left(\dfrac{U_{2n-2}[p_1(H_{2n})-p_1(H_{2n-2})]+D_{2n-1}[p_0(H_{2n})-p_0(H_{2n-2})]}{1-[p_1(H_{2n})-p_1(H_{2n-1})]}\right), \\ D_{2n+1}=D_{2n-1}+\left(\dfrac{D_{2n-1}[p_1(H_{2n-1})-p_1(H_{2n+1})]+U_{2n}[p_2(H_{2n-1})-p_2(H_{2n+1})]}{1-[p_1(H_{2n})-p_1(H_{2n+1})]}\right). \end{cases} \tag{8}$$

The derivation of Eqs. (8) is a little involved and we thus report it in Appendix A.

The magnetization as a function of the peak field is given by

$$\begin{aligned} M_{2n}=M_{2n-1}&+2U_{2n}^2[p_2(H_{2n})-p_2(H_{2n-1})] \\ &+4U_{2n}D_{2n-1}[p_1(H_{2n})-p_1(H_{2n-1})] \\ &+2D_{2n-1}^2[p_0(H_{2n})-p_0(H_{2n-1})] \end{aligned} \tag{9}$$

and a similar expression holds for $M_{2n+1}$.

In the limit $H_{2n-2}-H_{2n}\equiv dH\to 0$, $H_{2n}\to H^*$, and $H_{2n-1}\to -H^*$, the recursion relations in Eqs. (8) become a pair of differential equations,[27]

$$\begin{cases} \dfrac{\partial U}{\partial H^*}=\left(\dfrac{1}{1-\Omega}\right)[\rho(H^*)\tilde{D}+\rho(2J-H^*)U], \\ \dfrac{\partial \tilde{D}}{\partial H^*}=\left(\dfrac{1}{1-\Omega}\right)[\rho(H^*)U-\rho(2J-H^*)\tilde{D}], \end{cases} \tag{10}$$

where $\Omega\equiv\int_{-H^*}^{H^*}\rho(h')dh'$ and $\tilde{D}(H)\equiv D(-H)$. The boundary conditions are given by the conditional probabilities on the saturation loop [i.e., $U(J)=\tilde{D}(J)=U_0(J)=1/2$] and the solution reads

$$\begin{aligned} U(H^*)&=\tilde{D}(H^*) \\ &=\frac{1}{2}\exp\left(-\int_{H^*}^{J}\frac{\rho(h')+\rho(2J-h')}{1-\Omega(h')}dh'\right). \end{aligned} \tag{11}$$

Once the conditional probability $U$ is known, it is straightforward to compute the magnetization as a function of the peak field $H^*$ from Eq. (9), noting that $M(-H^*)=-M(H^*)$. Inner loops starting from the demagnetization curve [i.e., Eq. (9)] can also be computed exactly. In Fig. 1 we report the demagnetization curve and a few inner loops for a system with Gaussian random-field distribution with unit variance. The analytical results are compared with numerical simulations, performed on a lattice with $L=5\times 10^5$ spins, using a single realization of the disorder. The perfect agreement between the curves confirms that the magnetization is self-averaging, as assumed throughout the calculations.

## V. RAYLEIGH LAW

To analyze low-field hysteresis we first substitute in Eq. (9) $H_{2n}$ and $H_{2n-1}$ with $H^*$ and $-H^*$. If we start to reverse the field from $H_0=J$ and we cycle the field symmetrically around $H^*=0$, the process displays the symmetry $M(H^*)=-M(-H^*)$ and $U(H^*)=\tilde{D}(H^*)$. Thus we can reduce Eq. (9) to

$$M(H^*)=2U^2(H^*)\sum_{k=0}^{1}[p_k(H^*)-p_k(-H^*)]. \tag{12}$$

Now we can expand $M(H^*)$ around $H^*=0$. In this limit we have

$$[p_k(H^*)-p_k(-H^*)]\simeq\begin{cases} 2H^*\rho(2J) & \text{if } k=0,2, \\ 2H^*\rho(0) & \text{if } k=1, \end{cases} \tag{13}$$

and

$$U^2(H^*)\simeq U^2(0)\{1+2H^*[\rho(0)+\rho(2J)]\}. \tag{14}$$

Collecting Eqs. (13) and (14) in Eq. (12), we obtain $M\simeq aH^*+b(H^*)^2$ recovering the Rayleigh expression with

$$\begin{cases} a=4U^2(0)[\rho(0)+\rho(2J)], \\ b=4U^2(0)[\rho(0)+\rho(2J)]^2. \end{cases} \tag{15}$$

An expansion can also be performed for minor loops on the demagnetization curve (i.e., cycling $H$ between $\pm H^*$), yielding $M=(a+bH^*)H\pm b[(H^*)^2-H^2]/2$, which coincides with the Rayleigh law.

In Fig. 2(a) we report the values of $a$ and $b$ for a Gaussian distribution of random fields as a function of the disorder $R$, showing that both components of the susceptibility display a maximum in $R$. To identify the low and strong disorder behavior of the susceptibilities, we perform an asymptotic expansion and we obtain for $R\to\infty$ that $a\simeq 2/\sqrt{2\pi}R$ and $b\simeq 2/\pi R^2$. For $R\to 0$, we obtain: $a\simeq(1/e\pi J)e^{-J^2/2R^2}$ and $b\simeq(1/e\pi J\sqrt{2\pi})(1/R)e^{-J^2/2R^2}$. Finally in Fig. 2(b) we report

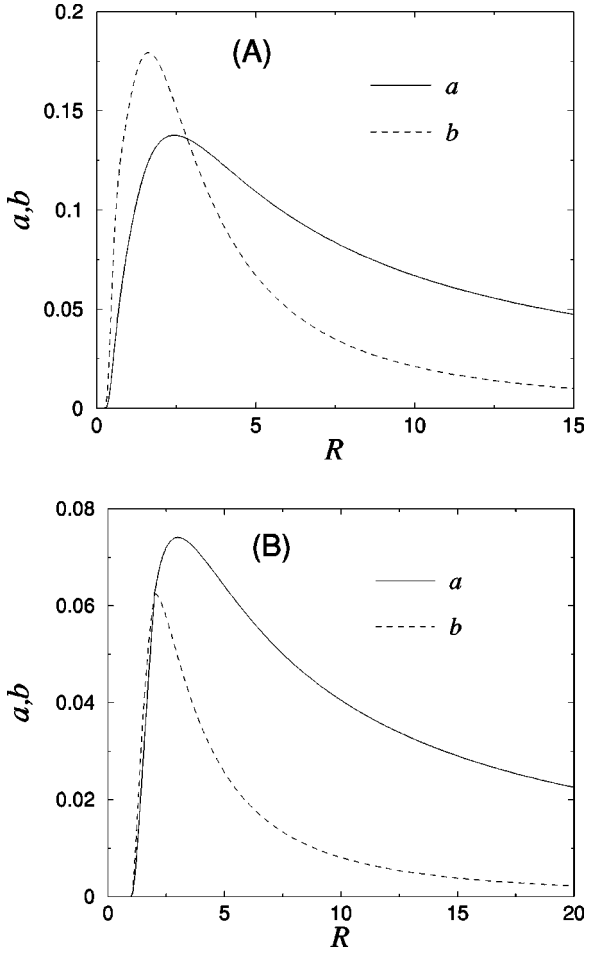


FIG. 2. The reversible susceptibility $a$ and the hysteretic coefficient $b$ computed exactly in $d=1$ for (a) a Gaussian distribution of random fields and (b) a rectangular distribution.

$a$ and $b$ obtained with a rectangular distribution of random fields. The derivation of these results is reported in Appendix B.

### VI. SIMULATIONS IN $D=2,3$

Next, we turn our attention to the high dimensional system, for which analytical results are not available. In order to obtain unambiguously the demagnetized state for a given realization of the disorder, one should perform a *perfect demagnetization*. This is done in practice by changing the field by precisely the amount necessary to flip the first unstable spin. In this way, the field is cycled between $-H^*$ and $H^*$ and $H^*$ is then decreased at the next cycle by precisely the amount necessary to have one avalanche less than in the previous cycle. This corresponds to decrease $H^*$ at each cycle by an amount $dH$, with $dH \to 0^+$. The perfect demagnetization algorithm allows us to obtain a precise characterization of the demagnetized state but it is computationally very demanding. Thus we resort to a different algorithm which performs an *approximate demagnetization*: instead of cycling the field between $-H^*$ and $H^*$ we just flip the field between these two values and then decrease $H^*$ by a fixed amount $dH$. We have checked that with a reasonably small $dH$ (i.e., $dH<10^{-3}$) the demagnetization curve is quite insensitive to the algorithm used.

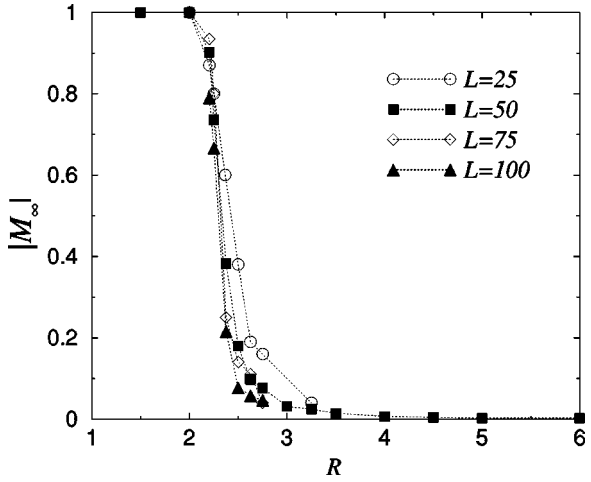


FIG. 3. The absolute value of the final magnetization $|M_\infty|$ as a function of $R$, obtained from numerical simulations in $d=3$. For strong disorder $|M_\infty|=0$ as expected, while for weak disorder the final magnetization coincides with the saturation value. The transition between the two types of behavior becomes sharper as the system size is increased.

As we discussed above, it is well established that in $d=3$ the saturation loops reveal a phase transition at $R_c \simeq 2.16$ for $J=1$ (Ref. 16) [the transition is not present in $d=1$, while in $d=2$ the issue is controversial (Ref. 16)]. We find that the transition is reflected also in the Rayleigh loops: in Fig. 3 we report the final magnetization $M_\infty$ computed using the demagnetization algorithm for different values of $R$. For strong disorder $R>R_c$, we see that $M_\infty \simeq 0$ as expected, but as $R<R_c$ the demagnetization curve tends to the saturation magnetization and $M_\infty \to \pm 1$. The transition becomes sharper as the system size is increased, indicating that demagnetization is possible only for $R>R_c$ (see also Ref. 24). We notice here that two scenarios are possible for $L \to \infty$ as $R \to R_c^-$. The first possibility is that $M_\infty$ scales continuously to zero as $(R_c-R)^\beta$ and the second is that the transition is discontinuous (i.e., $M_\infty \to M^*>0$). The present numerical results do not allow us to distinguish between these two cases, but a recent analysis of the RFIM on the Bethe lattice is in favor of the first alternative.[28]

From the demagnetization curve, the Rayleigh parameters can be estimated plotting $(M-M_\infty)/H$ vs $H$ and fitting the linear part of the curve close to $H=0$ (see Fig. 4). As we show in Fig. 4 the demagnetization curve is basically independent of the system size, once the magnetization has been shifted by $M_\infty$. Thus we expect that the Rayleigh parameters be also independent of $L$. In Fig. 5 we report the values of $a$ and $b$ obtained numerically in $d=2$ and $d=3$ for different values of $R$, using systems of sizes $(L=100)^2$ and $(L=50)^3$. The results are qualitatively similar to those obtained exactly in $d=1$: the curve displays a peak for intermediate disorder and a decrease to zero for weak and strong disorder.

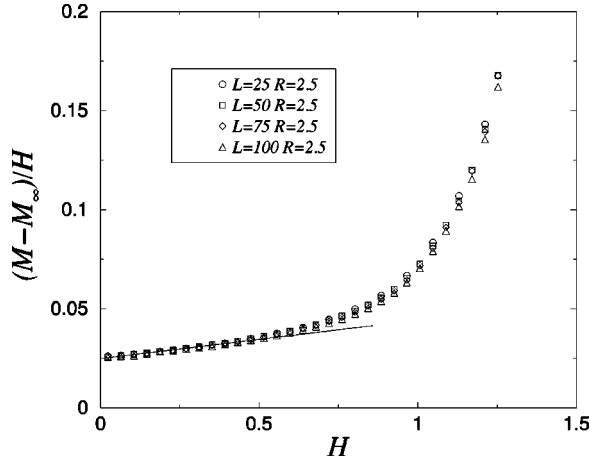


FIG. 4. The demagnetization curve can be used to obtain an estimate of the Rayleigh parameters. Notice the absence of system size dependence. These results are obtained in $d=3$.

## VII. DISCUSSION

In this paper we have discussed the demagnetization properties of the RFIM in $d=1,2,3$. In $d=1$ it is possible to compute exactly the demagnetization curve and obtain an expression for the Rayleigh parameters. We find that $a$ and $b$ display a peak in the disorder $R$. This result is confirmed by numerical simulations in $d=2,3$, where analytical results are not available. In addition, in $d=3$ the disorder induced phase transition strongly affects the demagnetization process: for $R<R_c$ it is not possible to demagnetize the system anymore.

It is interesting to compare our theoretical results with experiments on nanocrystalline materials. It has been reported that the initial susceptibility in several cases displays a peak as the heat treatment or the alloy composition are varied.[10–13] The peak is usually associated with changes in the microstructure, which induce a competition between the disorder present in grain anisotropies and intergrain interactions mediated by the amorphous matrix.[10] Notice that a similar behavior cannot be reproduced by Néel theory, where the initial susceptibility is decreasing with the width of the disorder potential.[5] On the other hand, we see here that the behavior is well captured by the RFIM, that allows us to analyze the the effect of the disorder-exchange ratio $R/J$. For weak disorder, we have a few large domains and the susceptibility is dominated by domain-wall dynamics. When the disorder is increased, the number of domains (and domain walls) also increases and so does the susceptibility. Increasing the disorder further leads to a complete breakup of the domains and the response is dominated by single spin flips in low random-field regions with a progressive decrease of the susceptibility.

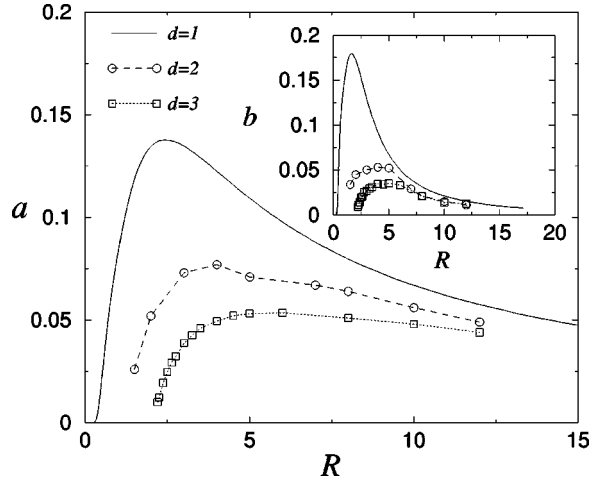


FIG. 5. The reversible susceptibility $a$ computed exactly in $d=1$ is compared with numerical results in $d=2$ and $d=3$. In the inset we show a similar plot for the parameter $b$.

A detailed understanding of the demagnetization process and low-field hysteresis has important implications also from a purely theoretical point of view. When a disordered system is demagnetized, it explores a complex energy landscape until it finds a metastable minimum. It would be interesting to compare the statistical properties of the demagnetized state with those of the ground state of the system.[25] The analysis of the ground state of disordered systems has received wide attention in the past few years, due to the connections with general optimization problems, and the RFIM is one of the typical models used to test ground-state algorithms.[29] Demagnetization could provide a relatively simple way to obtain a low-energy state that can be useful for optimization procedures. We are currently pursuing investigations along these lines.[30]

## ACKNOWLEDGMENTS

This work was supported by the INFM PAIS-G project on ''Hysteresis in disordered ferromagnets.'' We thank M. J. Alava, G. Bertotti, F. Colaiori, and A. Gabrielli for useful discussions and remarks.

## APPENDIX A: DERIVATION OF THE RECURSION RELATIONS

Here, we derive recursion relations for the conditional probabilities $U_{2n}$ and $D_{2n+1}$ as a function of the previous magnetization history. Let us first consider the case of $D_{2n+1}$: the field from $H_{2n-1}$ reaches $H_{2n}$ and is then decreased again up to $H_{2n+1}$. The weight of the fraction of spins that at field $H_{2n+1}$ flip *down* before their neighbor is given by

$$D_{2n+1}=D_{2n-1}-\zeta_{2n}+\zeta_{2n+1}, \tag{A1}$$

where $\zeta_{2n}$ is the weight of the fraction of spins that were *down* at $H_{2n-1}$ before a fixed nearest neighbor and flip *up* at $H_{2n}$, while $\zeta_{2n+1}$ is the weight of the fraction of spins contributing to $\zeta_{2n}$ which flip again *down* at $H_{2n+1}$.

To compute $\zeta_{2n}$, we consider the spins that at the field $H_{2n-1}$ are *down* before their neighbor (for instance, we can say that the spin $i$th is *down* before the spin in site $i-1$) and are *up* at the field $H_{2n}$. Since we fixed *up* the spin in site $i-1$, the spin in site $i+1$ can be either *up* or *down*. If the spin in $i+1$ is *up* when the spin $i$ flips *up*, it contributes to $\zeta_{2n}$ with

$$U_{2n}[p_2(H_{2n})-p_2(H_{2n-1})].$$

If the spin in site $i+1$ is *down* when the spin $i$ flips *up*, we obtain

$$D_{2n-1}[p_1(H_{2n})-p_1(H_{2n-1})].$$

Indeed, $[p_n(H_{2n})-p_n(H_{2n-1})]$ is the probability that a spin with $n$ *up* nearest neighbors is *up* at $H_{2n}$ but not at $H_{2n-1}$, while $D_{2n-1}, U_{2n}$ are, respectively, the conditional probabilities that the spin in site $i+1$ is *down* or *up* if the spin in site $i$ is *down*. Adding the two contributions, we obtain

$$\zeta_{2n}=\{D_{2n-1}[p_1(H_{2n})-p_1(H_{2n-1})] + U_{2n}[p_2(H_{2n})-p_2(H_{2n-1})]\}. \tag{A2}$$

The derivation of $\zeta_{2n+1}$ follows similar steps: we count the spins that are *up* at $H_{2n}$ and are again *down* at $H_{2n+1}$. If the spin in the site $i+1$ is *up* at $H_{2n+1}$, the spin in $i$ is *up* at $H_{2n}$ and is *down* at $H_{2n+1}$ with probability

$$U_{2n}[p_2(H_{2n})-p_2(H_{2n+1})].$$

Finally, we analyze the case in which the spin in site $i+1$ is already *down* when the spin $i$ flips *down*. The weight of this configuration is

$$D_{2n+1}[p_1(H_{2n})-p_1(H_{2n+1})],$$

so that $\zeta_{2n+1}$ is given by

$$\zeta_{2n+1}=\{U_{2n}[p_2(H_{2n})-p_2(H_{2n+1})] + D_{2n+1}[p_1(H_{2n})-p_1(H_{2n+1})]\}. \tag{A3}$$

Substituting these two expressions in Eq. (A1) we obtain the second of Eqs. (8). We can then derive a similar equation for $U_{2n}$ [first of Eqs. (8)] following the same method as the one employed above to calculate $D_{2n+1}$.

## APPENDIX B: THE CASE OF THE RECTANGULAR DISTRIBUTION

It is also instructive to consider the case of a rectangular distribution of random fields [i.e., $\rho(x)=1/2\Delta$ if $|x|<\Delta$ and zero otherwise], since all the calculations can be carried out explicitly. As usual, we cycle the field around $H=0$ and we take $H_0=J$. The calculation should be divided in several cases, depending on the value of $\Delta$.

(i) For $\Delta \geqslant 3J$, we have $\rho(x)=\rho(2J-x)=1/2\Delta$, so that $p_k(H^*)-p_k(-H^*)=H^*/\Delta$ and Eq. (11), reduces to

$$U^2(H^*)=\frac{1}{4}\left(\frac{\Delta-J}{\Delta-H^*}\right)^2. \tag{B1}$$

Inserting these results in Eq. (12), we obtain

$$M(H^*)=\left(\frac{\Delta-J}{\Delta-H^*}\right)^2\frac{H}{\Delta}. \tag{B2}$$

Expanding Eq. (B2), we obtain the values for $a$ and $b$

$$\begin{cases} a=\dfrac{1}{\Delta}\left[1-\dfrac{J}{\Delta}\right]^2, \\ b=2\dfrac{1}{\Delta^2}\left[1-\dfrac{J}{\Delta}\right]^2. \end{cases} \tag{B3}$$

(ii) For $2J<\Delta<3J$, $U^2(0)$ is still given by Eq. (B1) but $p_k(H^*)$ differs from the previous case. The magnetization is now given by

$$\begin{cases} M(H^*)=\left(\dfrac{\Delta-J}{(\Delta-H^*)}\right)^2\dfrac{3H^*-2J+\Delta}{4\Delta} \\ \text{if } H^*>\Delta-2J, \\ M(H^*)=\left(\dfrac{\Delta-J}{(\Delta-H^*)}\right)^2\dfrac{H}{\Delta} \\ \text{if } H^*<\Delta-2J. \end{cases} \tag{B4}$$

The expansion around $H^*$ is thus still given by Eq. (B3).

(iii) The behavior for $J<\Delta<2J$ is again different: close to $H^*=0$ the peak magnetization is not given by Eq. (12), but for $H^*<2J-\Delta$ can be written as

$$M(H^*)=\frac{(\Delta-J)^2H^*}{4J\Delta(\Delta-H^*)}, \tag{B5}$$

so that expanding we obtain

$$\begin{cases} a=\dfrac{(\Delta-J)^2}{4\Delta^2J}, \\ b=\dfrac{(\Delta-J)^2}{2\Delta^3J}. \end{cases} \tag{B6}$$

(iv) Finally for $\Delta<J$ there is no hysteresis and thus the Rayleigh law is not defined.


[1] L. Rayleigh, Philos. Mag., Suppl. **23**, 225 (1887).

[2] G. Bertotti, *Hysteresis in Magnetism* (Academic Press, San Diego, 1998).

[3] D. Damjanovic, J. Appl. Phys. **82**, 1788 (1997). For a review, see Rep. Prog. Phys. **61**, 1267 (1998).

[4] D. Bolten, U. Böttger, T. Schneller, M. Grossman, O. Lohse, and R. Waser, Appl. Phys. Lett. **77**, 3830 (2000).

[5] L. Néel, Cah. Phys. **12**, 1 (1942).

[6] K. H. Pfeffer, Phys. Status Solidi **21**, 857 (1967).

[7] R. Vergne, Z. Blazek, and J. L. Porteseil, Phys. Status Solidi A **25**, 171 (1974).

[8] H. Kronmüller and T. Reininger, J. Magn. Magn. Mater. **112**, 1 (1992).

[9] A. Magni, C. Beatrice, G. Durin, and G. Bertotti, J. Appl. Phys. **86**, 3253 (1999).

[10] G. Herzer, in *Handbook of Magnetic Materials*, edited by K. H. J.

Buschow (Elsevier, Amsterdam, 1997), Vol. 10, p. 415.
[11] K. Suzuki, A. Makino, A. Inoue, and T. Masumoto, J. Appl. Phys. **70**, 6232 (1991).
[12] M. S. Leu and T. S. Chin, J. Appl. Phys. **81**, 4051 (1997).
[13] S. H. Lim, W. K. Pi, T. H. Noh, H. J. Kim, and I. K. Kang, J. Appl. Phys. **73**, 6591 (1993).
[14] J. P. Sethna, K. Dahmen, S. Kartha, J. A. Krumhansl, and J. D. Shore, Phys. Rev. Lett. **70**, 3347 (1993).
[15] K. Dahmen and J. P. Sethna, Phys. Rev. B **53**, 14 872 (1996).
[16] O. Perkovic, K. A. Dahmen, and J. P. Sethna, Phys. Rev. B **59**, 6106 (1999).
[17] E. Vives and A. Planes, Phys. Rev. B **50**, 3839 (1994); **63**, 134431 (2001).
[18] R. da Silveira and M. Kardar, Phys. Rev. E **59**, 1355 (1999).
[19] A. Berger, A. Inomata, J. S. Jiang, J. E. Pearson, and S. D. Bader, Phys. Rev. Lett. **85**, 4176 (2000).
[20] P. Shukla, Physica A **233**, 235 (1996).
[21] P. Shukla, Phys. Rev. E **62**, 4725 (2000).
[22] D. Dhar, P. Shukla, and J. P. Sethna, J. Phys. A **30**, 5259 (1997).
[23] P. Shukla, Phys. Rev. E **63**, 027 102 (2001).
[24] J. H. Carpenter, K. A. Dahmen, J. P. Sethna, G. Friedman, S. Loverde, and A. Vanderveld, J. Appl. Phys. **89**, 6799 (2001).
[25] G. Bertotti and M. Pasquale, J. Appl. Phys. **67**, 5255 (1990).
[26] Notice that these equations are only valid for $|H_n| \leqslant H_0 - 2J$.
[27] For instance, the limit can be taken choosing $H_n = (-1)^n(1-\epsilon)^n J$ and then expanding all the quantities for $\epsilon \to 0^+$.
[28] F. Colaiori, A. Gabrielli, and S. Zapperi, cond-mat/0112190 (unpublished).
[29] M. Alava, P. Duxbury, C. Moukarzel, and H. Rieger, in *Phase Transitions and Critical Phenomena*, edited by C. Domb and J. Lebowitz (Academic Press, San Diego, 2001), Vol. 18.
[30] A recent investigation of such a ''hysteretic optimization'' can be found in G. Zarand, F. Pazmandi, K. F. Pal, and G. T. Zimanyi, cond-mat/0109359 (unpublished).